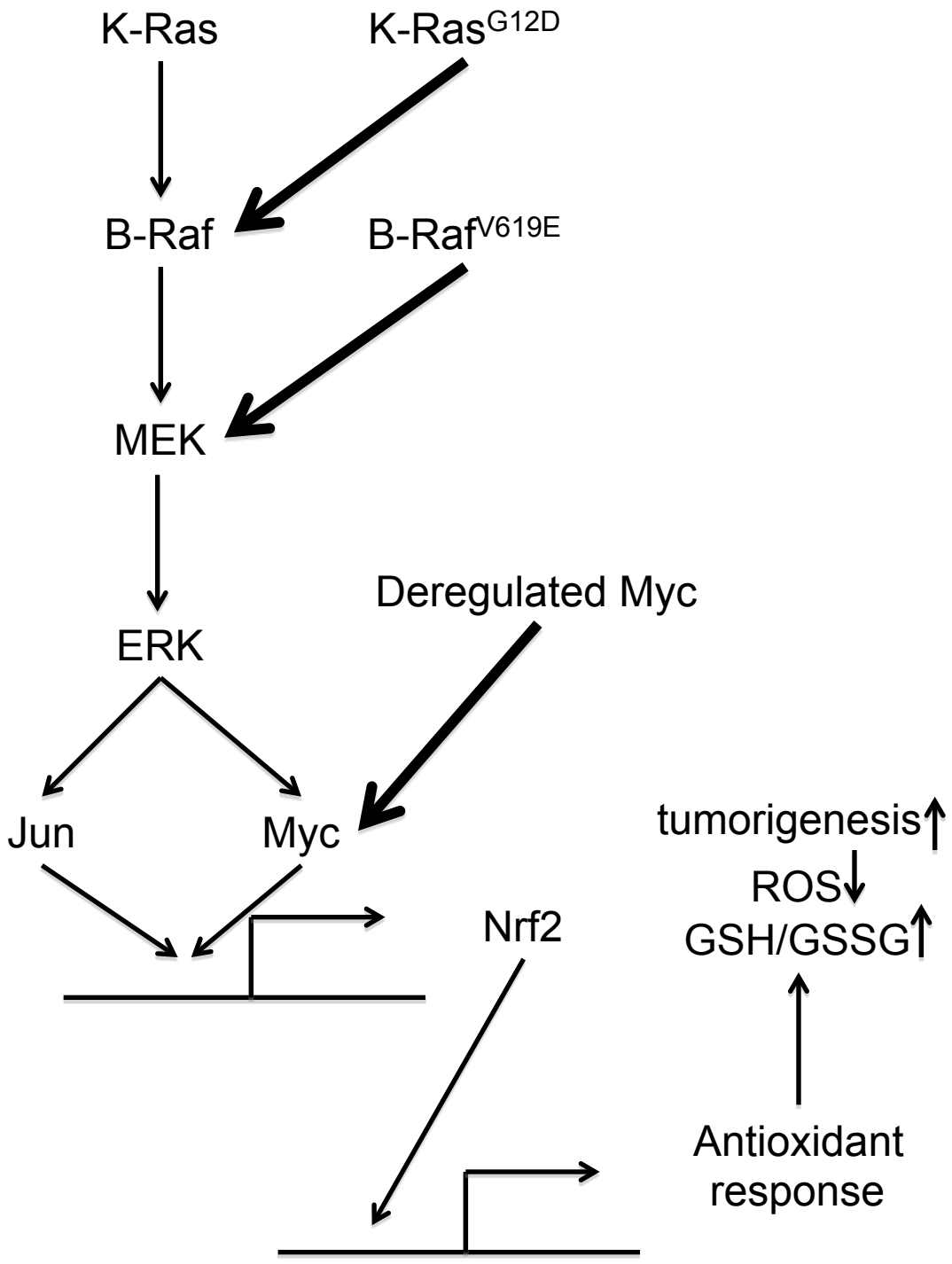

Supplementary Figure 1: Model.

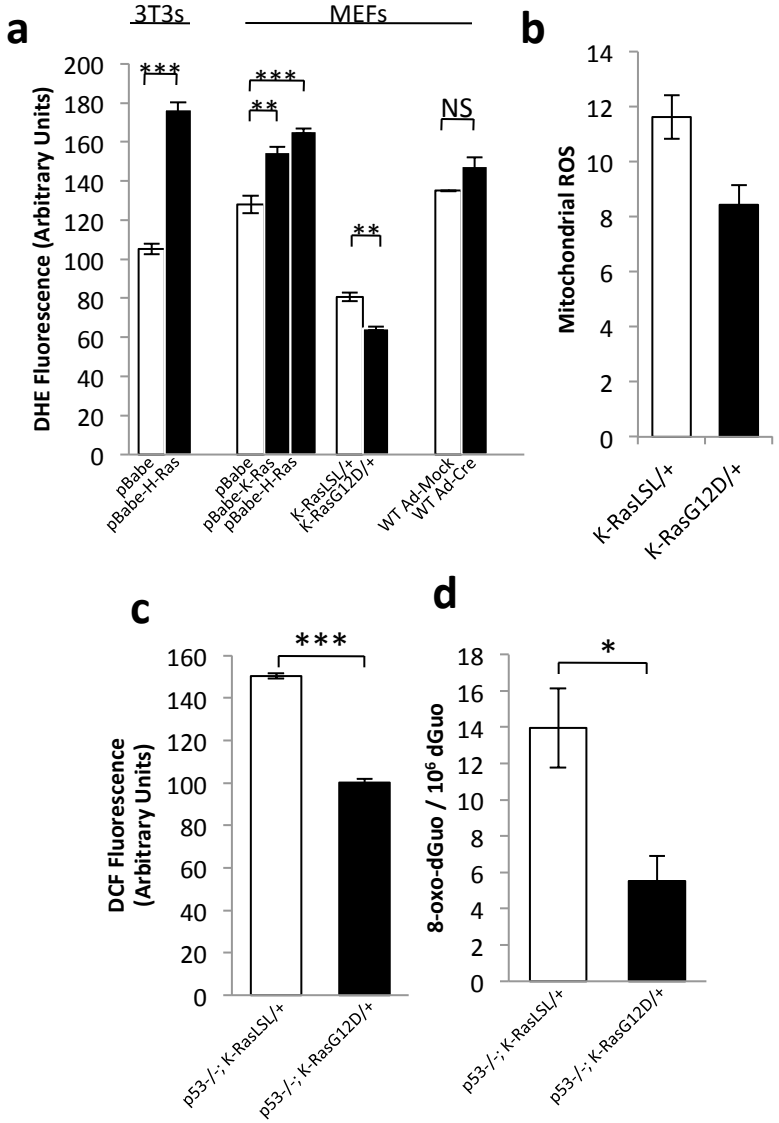

Supplementary Figure 2: Endogenous expression of oncogenic K-Ras decreases ROS. a, Overexpression of mutant Ras elevates whereas endogenous K-Ras^{G12D} decreases intracellular superoxide levels, as determined by dihydroethidium (DHE) staining. **b,** Endogenous expression of K-Ras^{G12D} decreases mitochondrial ROS. Mitochondrial ROS was determined by the MitoSOX Red mitochondrial superoxide indicator, and normalized to Mitotracker Green fluorescence. **c,** K-Ras$^{LSL/+}$; p53$^{-/-}$ and K-Ras$^{G12D/+}$; p53$^{-/-}$ MEFs were assayed for hydrogen peroxide levels by DCF staining. **d,** K-Ras$^{LSL/+}$; p53$^{-/-}$ and K-Ras$^{G12D/+}$; p53$^{-/-}$ MEFs were assayed for 8-oxo-dGuo levels by MS.

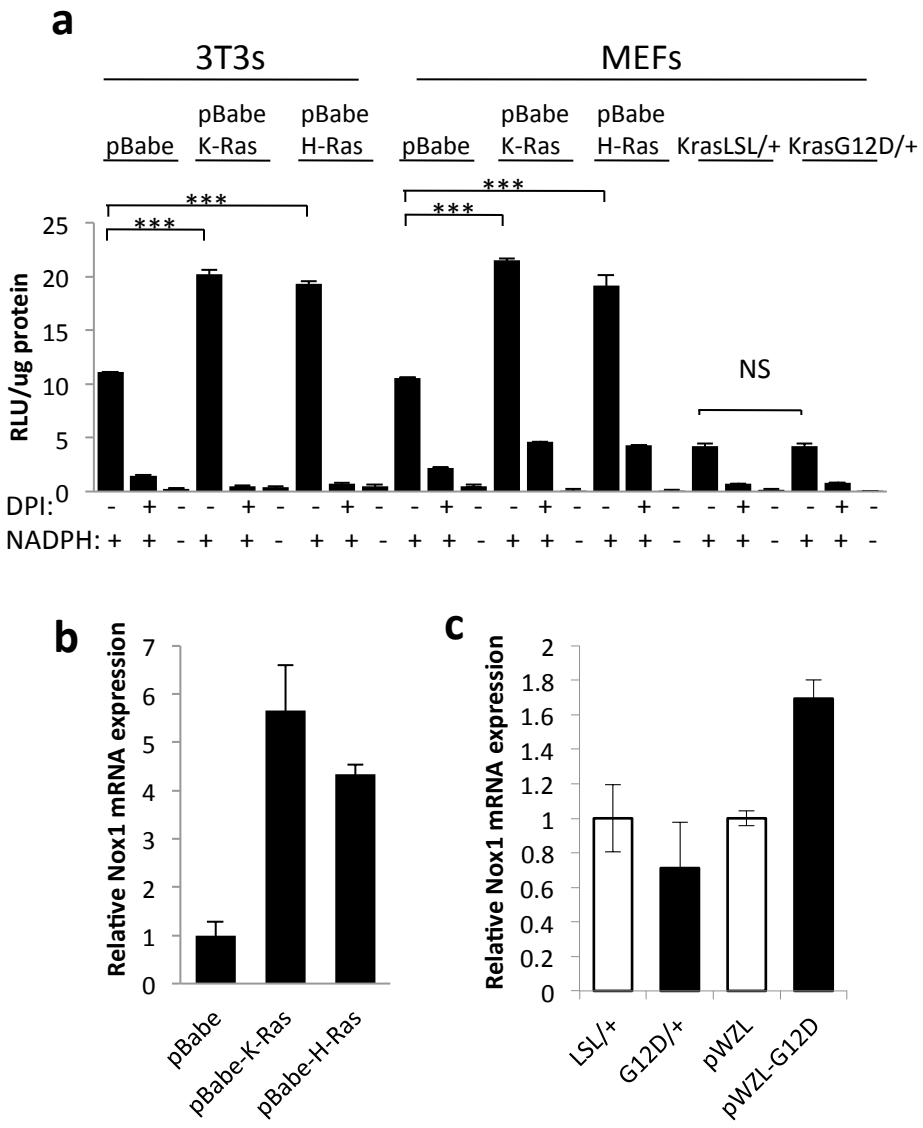

Supplementary Figure 3: Nox activity is increased by overexpression of oncogenic H- and K-Ras in NIH3T3s and MEFs, but unchanged by endogenous K-Ras^{G12D} expression. a, Nox activity was assayed by an NADPH-dependent lucigenin chemiluminescence assay. Specificity was determined by both sensitivity to the Nox inhibitor DPI (10uM) and dependence on NADPH. Results are representative of three independently performed experiments. **b,** Nox1 mRNA expression following ectopic expression of K-Ras^{G12D} and H-Ras^{V12} in NIH3T3s. **c,** Nox1 mRNA expression following endogenous (G12D/+ vs LSL/+) and ectopic (pWZL-G12D vs pWZL) expression of K-Ras^{G12D} in primary MEFs.

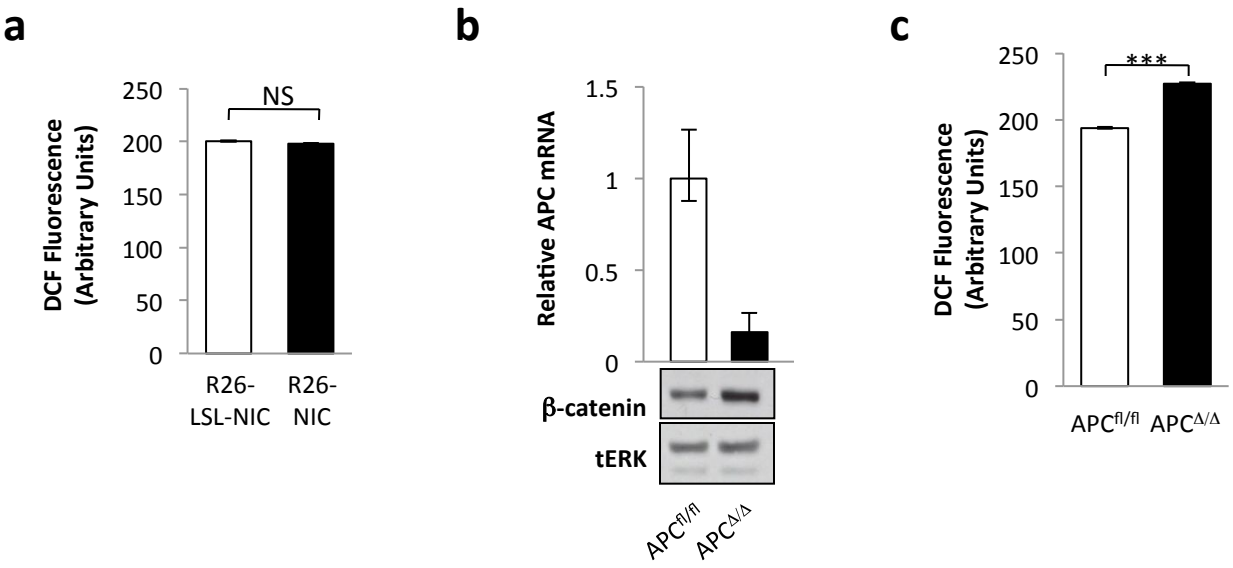

Supplementary Figure 4 : The activation of Notch and β-Catenin do not decrease ROS levels. a, Active Notch does not affect ROS, as determined by DCF oxidation. R26-LSL-NIC MEFs were infected with Ad-mock and Ad-cre and assayed for DCF after 4 days. **b-c,** Active β-catenin does not decrease ROS levels or affect Nrf2 activity. **b,** Deletion of APC induces accumulation of β-catenin. APCfl/fl MEFs were infected with Ad-mock (APCfl/fl) or Ad-cre (APC Δ/Δ) and immunoblotted for β-catenin after 4 days. Deletion of APC was verified by taqman gene expression assays. **c,** ROS levels 4 days after adenoviral infection, as determined by DCF oxidation. Results are representative of three independently performed experiments.

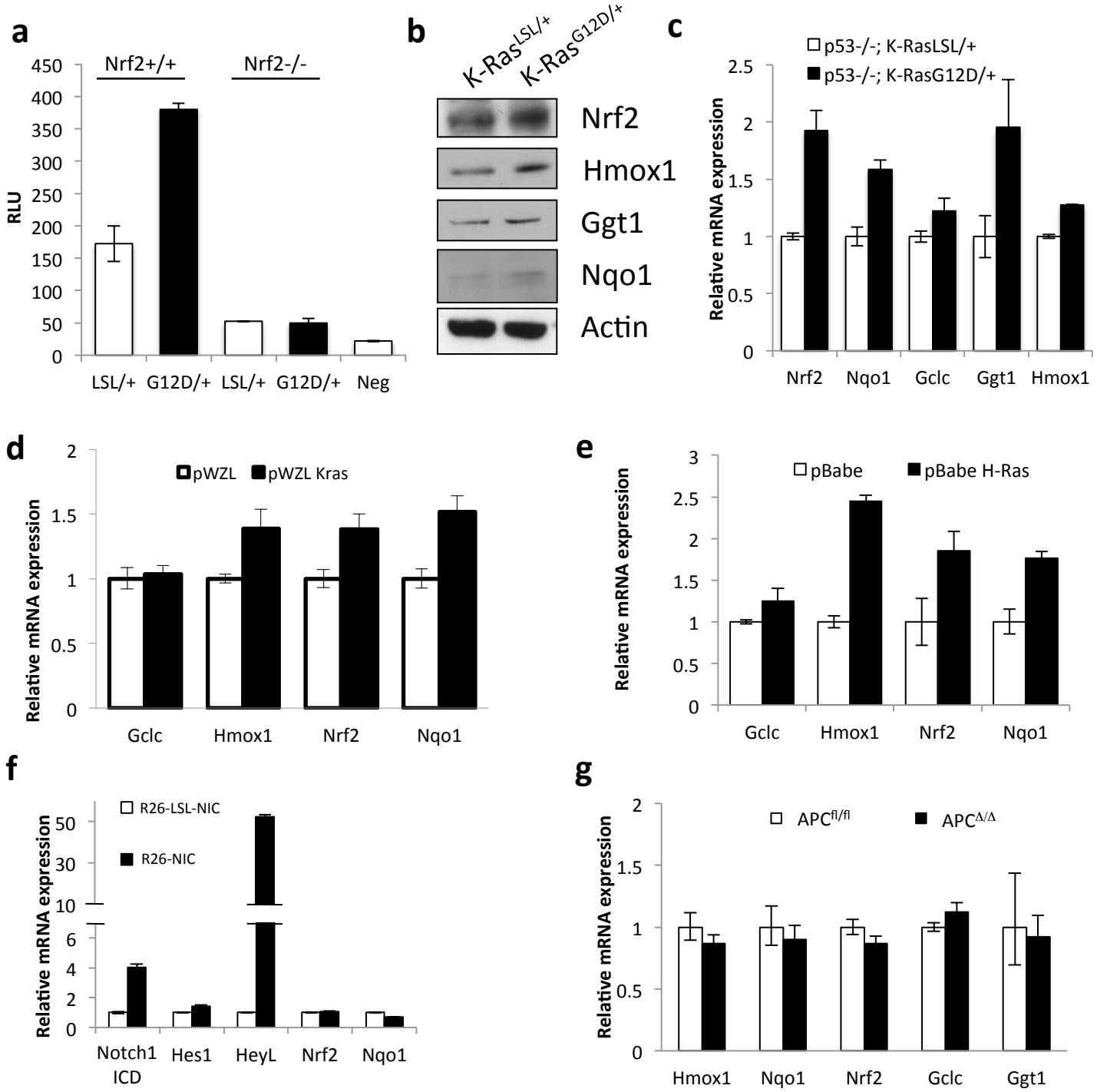

Supplementary Figure 5: Ectopic and endogenous expression of K-Ras^{G12D} and ectopic H-Ras^{V12}, but not Notch1 or β-Catenin, induces expression of Nrf2 and its target genes. a, Activation of an antioxidant response element reporter following expression of K-Ras^{G12D}, which is Nrf2 dependent. MEFs were infected with lentiviruses encoding ARE-luciferase, harvested, and assayed for luciferase activity. MEFs lacking the reporter (neg) were included as controls. **b,** Western blot of Nrf2 and Nrf2 target genes following expression of endogenous K-Ras^{G12D}. **c,** Determination of Nrf2 expression and activity following endogenous K-Ras^{G12D} expression in p53-/- MEFs. **d,** Nrf2 and target gene expression following ectopic K-Ras^{G12D} expression in primary MEFs. **e,** Nrf2 and target gene expression following ectopic H-Ras^{V12} expression in primary MEFs. **f,** Analysis of Notch activity and antioxidant gene expression following expression of NotchIC. R26-LSL- NIC MEFs were infected with Ad-mock or Ad-cre and assayed for gene expression after 4 days. **g,** Analysis of antioxidant gene expression following deletion of APC. APC fl/fl MEFs were infected with Ad-mock or Ad-cre and assayed for gene expression after 4 days. Gene expression was determined with taqman gene expression assays, and normalized to the expression of actin.

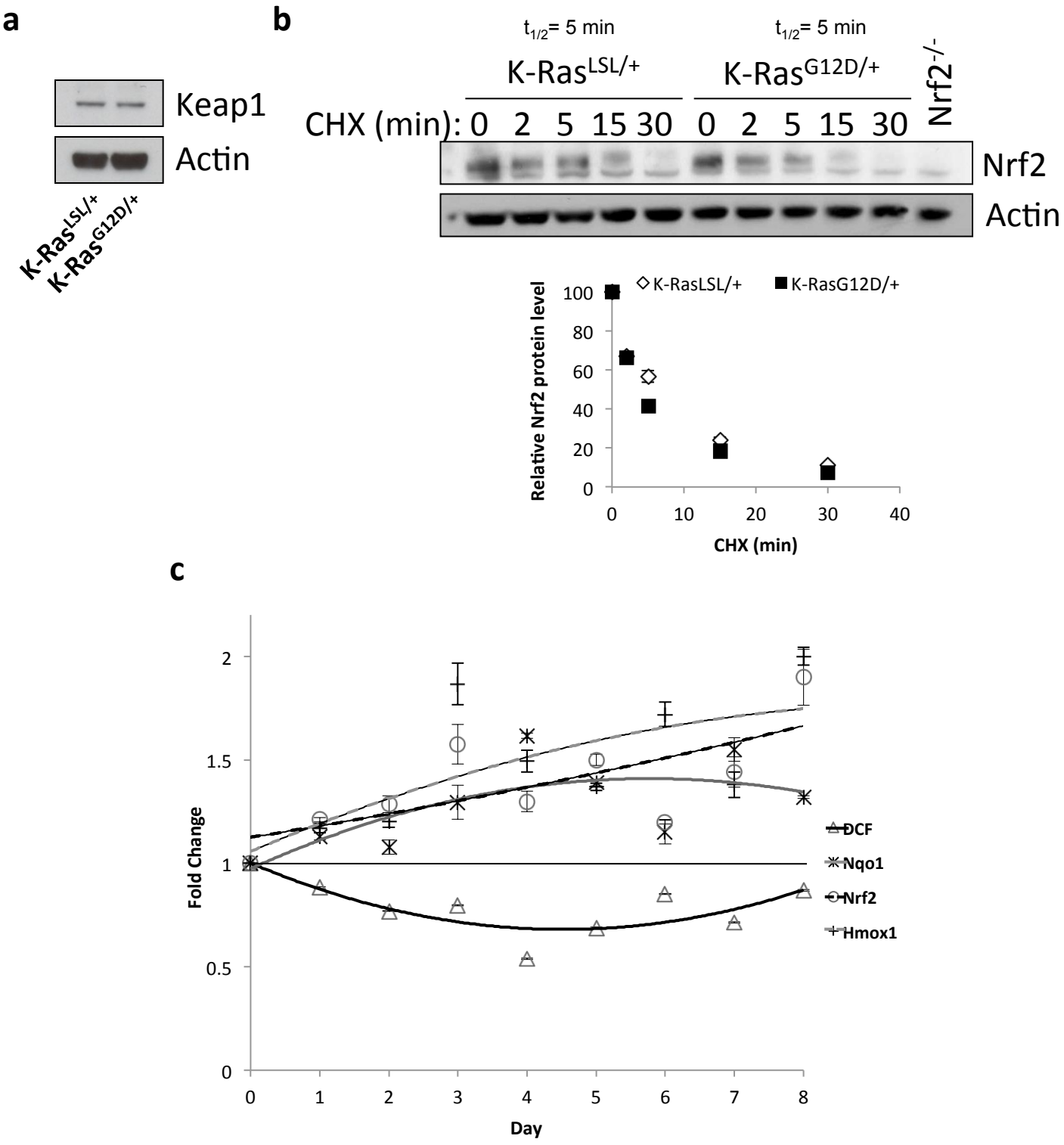

Supplementary Figure 6: Keap1 and ROS-independent activation of Nrf2 by K-Ras^{G12D}. a, Western blot of Keap1 and actin in K-Ras$^{LSL/+}$ and K-Ras$^{G12D/+}$ MEFs. **b,** Determination of Nrf2 stability. Total cell lysates from K-Ras$^{LSL/+}$ and K-Ras$^{G12D/+}$ MEFs treated with 25 ug/mL cycloheximide for the indicated times were subjected to immunoblot analysis with anti-Nrf2 antibody. Densitometry represents the average of two experiments. Error bars represent SEM. **c,** Time-course of DCF oxidation and Nrf2, Hmox1, and Nqo1 mRNA expression following expression of K-Ras^{G12D}. Expression of Nrf2, Hmox1, and Nqo1 was normalized to actin expression, and DCF and mRNA results were normalized to LSL-K-RasG12D MEFs infected with Ad-mock.

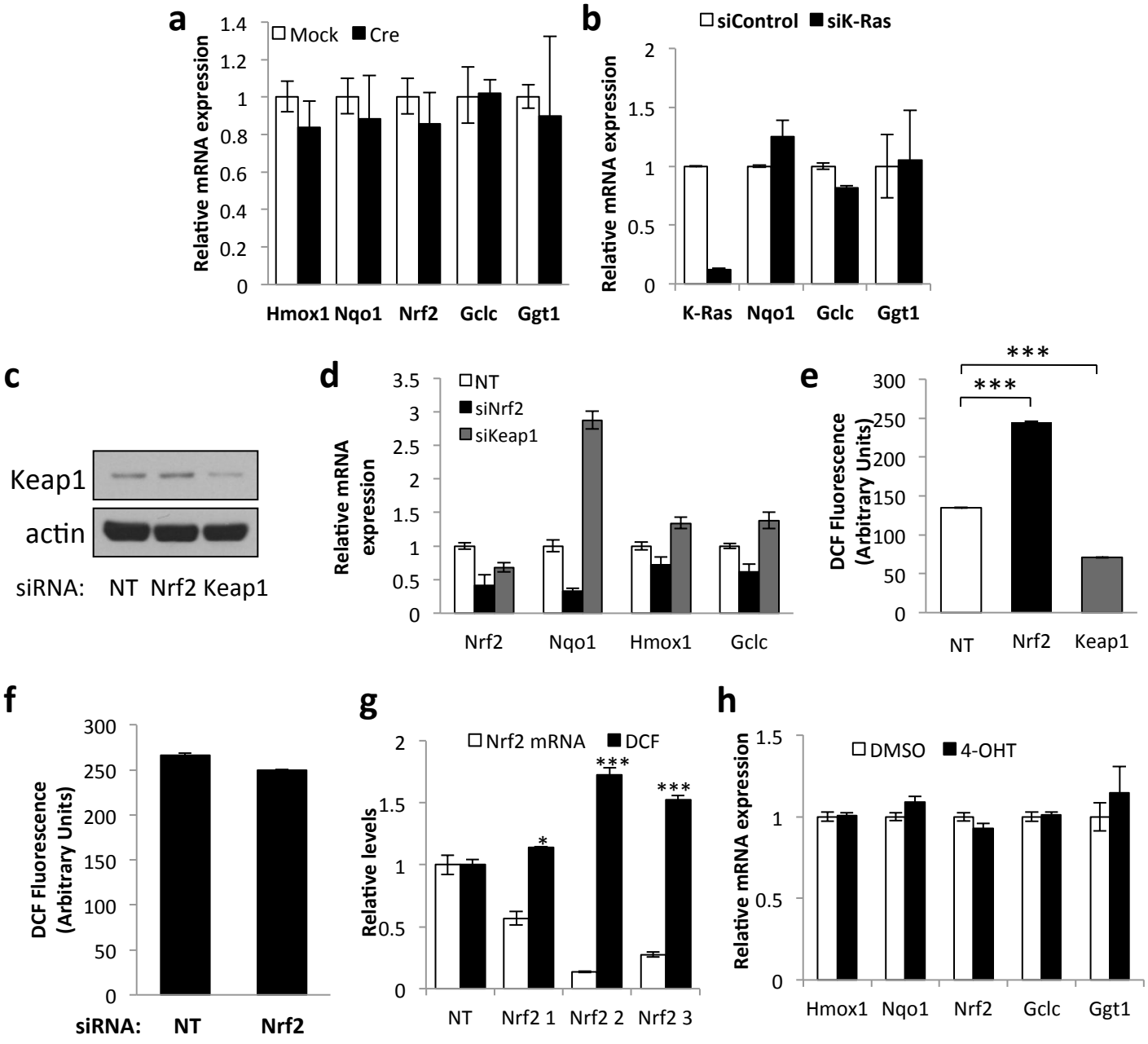

Supplementary Figure 7: Activation of Nrf2 is not due to expression of cre recombinase, modulation of wild-type K-Ras levels, or treatment with 4-OHT. a, Expression of cre recombinase does not induce antioxidant response gene expression in wild-type MEFs. Wild-type MEFs were infected with adenoviral-mock or adenoviral-cre and assayed for antioxidant gene expression 96 hours later. **b,** Induction of antioxidant response is independent of wild-type K-Ras gene dosage. Wild-type MEFs were transfected with non-targeting (NT) or K-Ras (siKras) siRNA and assayed for antioxidant gene expression 72 hours later. **c,** Verification of Keap1 knockdown. MEFs were immunoblotted for Keap1 and actin. **d,** Activation of Nrf2 affects antioxidant gene levels, but not Nrf2 transcription. Nrf2 and target gene mRNA was determined with taqman gene expression assays and normalized to actin. mRNA expression is shown relative to non-targeting siRNA transfected MEFs. **e,** Modulation of Nrf2 activity affects ROS levels. MEFs transfected with NT, Nrf2 or Keap1 siRNA were assed for DCF oxidation. **f,** Nrf2 siRNA does not affect ROS levels in $Nrf2^{-/-}$ MEFs. $Nrf2^{-/-}$ MEFs were transfected with NT or Nrf2 siRNA and assayed for ROS by DCF oxidation after 48 hours. **g,** Inverse correlation between Nrf2 mRNA levels and ROS levels in K-RasG12D/+ MEFs. K-RasG12D/+ MEFs were transfected with NT siRNA, or 3 siRNAs targeting Nrf2. **h,** 100nM 4-OHT does not affect Nrf2 activity. Wild-type MEFs were treated with DMSO or 100nM 4-OHT and assayed for antioxidant gene transcription after 24 hours. Results are shown relative to MEFs treated with DMSO. Results are representative of three independently performed experiments.

a

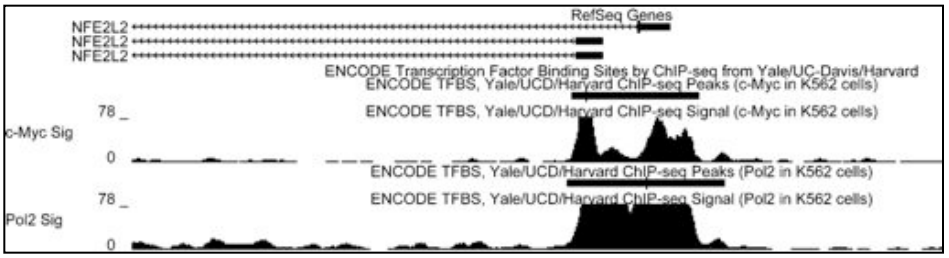

b

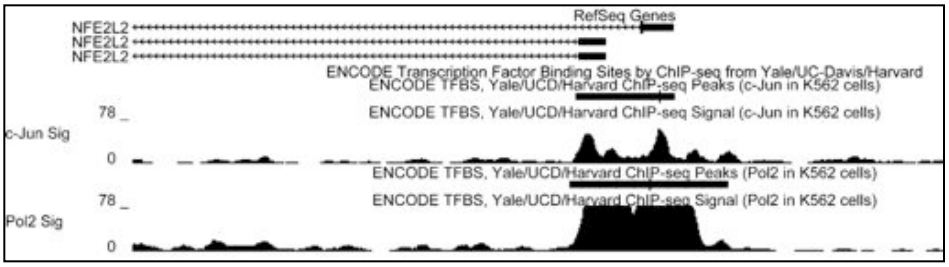

Supplementary Figure 8: Jun and Myc bind directly to the Nrf2 promoter. a, ChIP-seq data from the ENCODE Consortium demonstrates Myc binding to the Nrf2 promoter. Myc binding occurs at the transcriptional start site in exon1 of Nrf2 and overlaps with sites of RNA pol II binding. **b,** ChIP-seq data from the ENCODE Consortium demonstrates Jun binding to the Nrf2 promoter. Jun binding occurs at the transcriptional start site in exon1 of Nrf2 and overlaps with RNA pol II binding. Black bars denote positive signal above background.

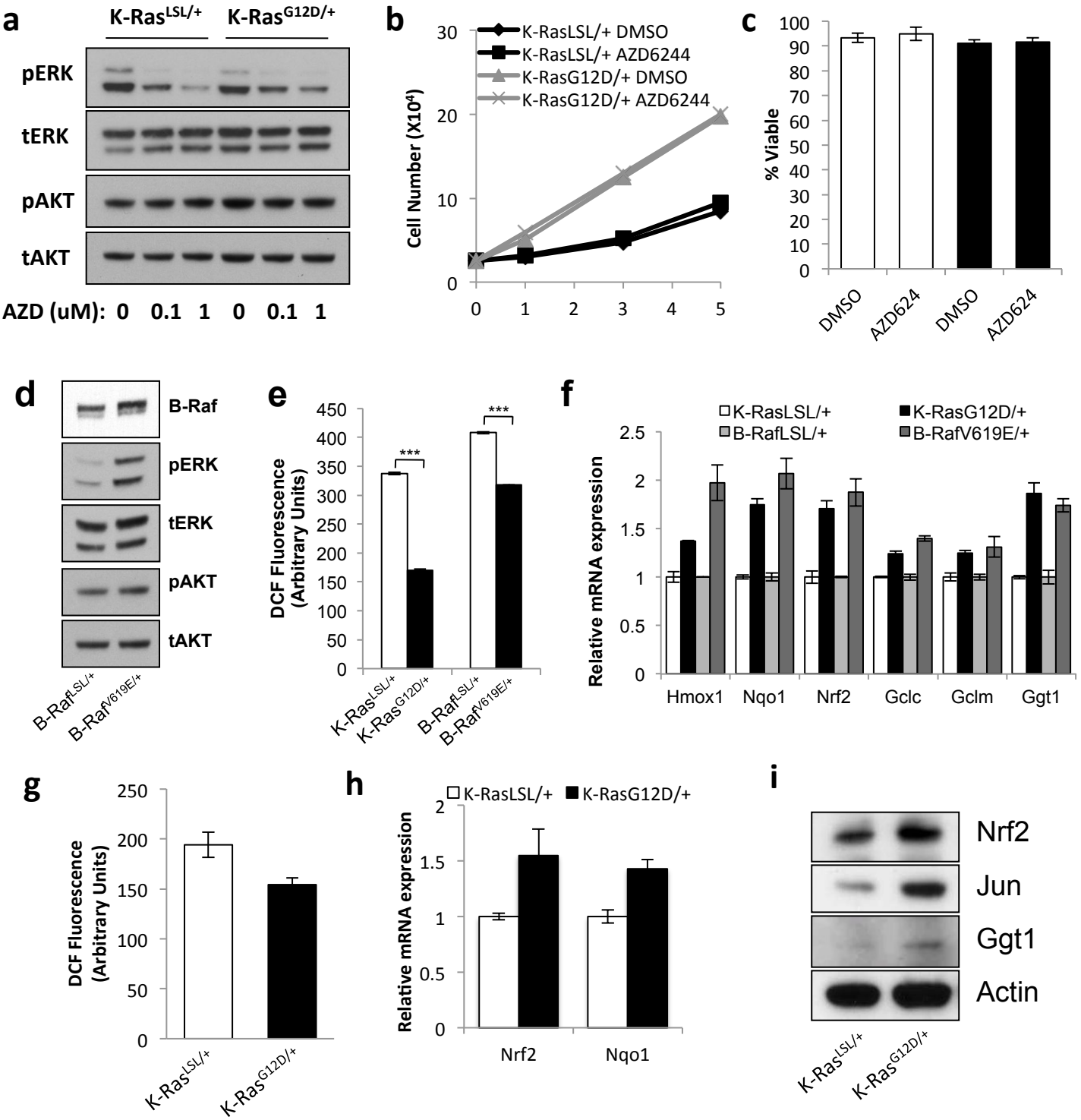

Supplementary Figure 9: Regulation of Nrf2 by Raf/MEK/ERK signaling, but not p38MAPK. a, Dose response of AZD6244 to inhibit MAPK signalling in MEFs. Treatment of K-Ras$^{LSL/+}$ and K-Ras$^{G12D/+}$ MEFs with AZD6244 inhibits MEK. Cells were treated for 2 hours with 0, 0.1 or 1uM AZD6244 and immunoblotted for pERK. There was no appreciable effect on pAKT, demonstrating the specificity of the inhibitor. **b,** AZD6244 does not affect cellular proliferation at 0.1uM. **c,** AZD6244 does not affect cell survival at 0.1uM. Cell survival was determined by trypan blue staining. **d-f,** Expression of B-Raf^{V619E} activates Nrf2 and lowers ROS. **d,** Western blot showing ERK but not AKT activation in LSL-B-Raf^{V619E} MEFs infected with Ad-mock (B-Raf$^{LSL/+}$) and Ad-cre (B-Raf$^{V619E/+}$). **e,** Comparison of the effects of K-Ras^{G12D} and B-Raf^{V619E} on ROS levels. **f,** Comparison of the effects of K-Ras^{G12D} and B-Raf^{V619E} on antioxidant gene expression. **g-i,** p38a does not mediate Nrf2 activation by K-Ras^{G12D}. **g,** p38a$^{-/-}$; K-Ras$^{LSL/+}$ and p38a$^{-/-}$; K-Ras$^{G12D/+}$ MEFs were assessed for DCF oxidation. **h,** p38a$^{-/-}$; K-Ras$^{LSL/+}$ and p38a$^{-/-}$; K-Ras$^{G12D/+}$ MEFs were assessed for Nrf2 expression and activity. **i,** Western blot of Nrf2, Jun and the Nrf2 target gene Ggt1 following expression of endogenous K-Ras^{G12D} in p38a$^{-/-}$ MEFs. Results are representative of three independently performed experiments.

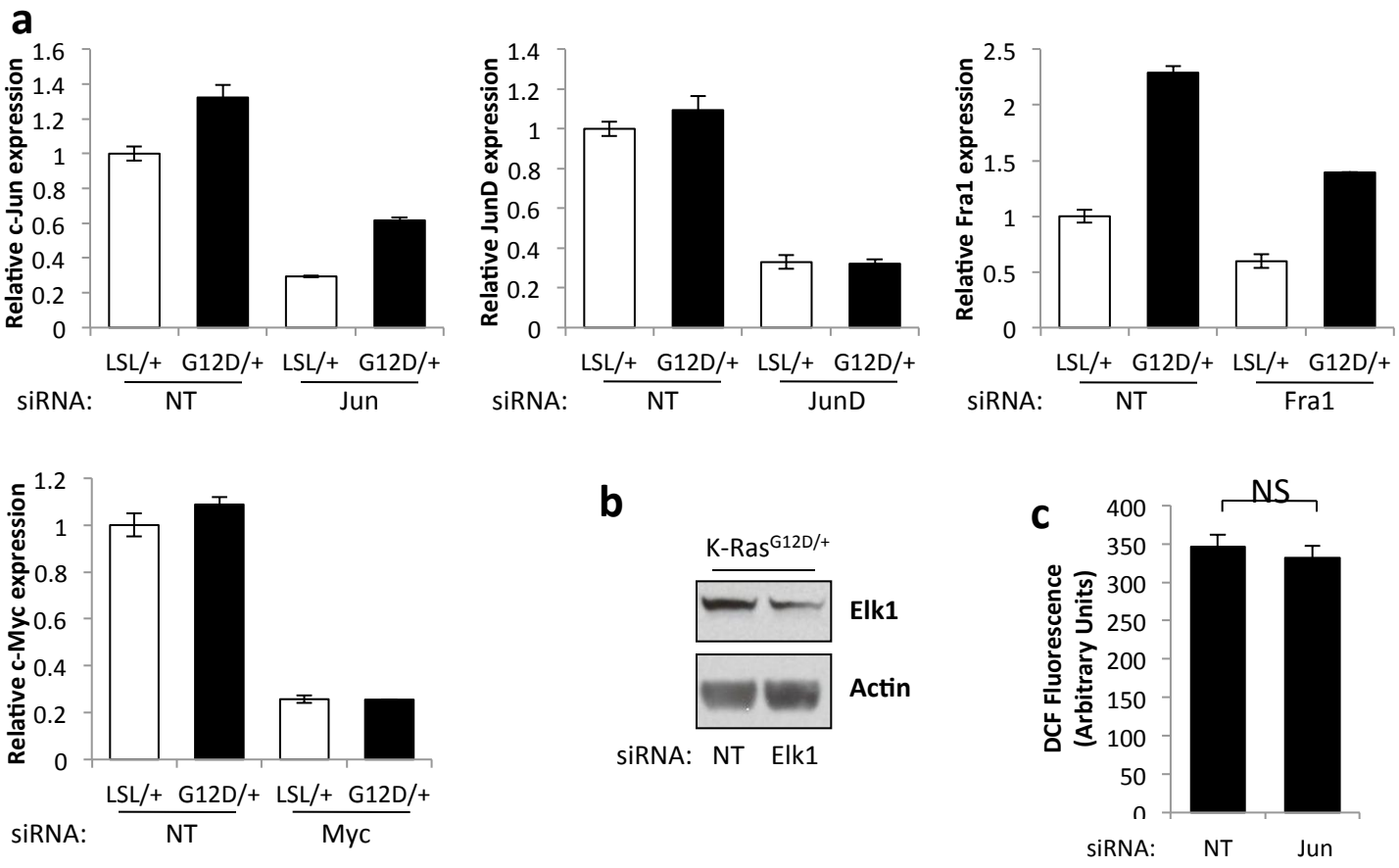

Supplementary Figure 10: Verification of siRNA efficacy. a, K-Ras$^{LSL/+}$ and K-Ras$^{G12D/+}$ MEFs were transfected with NT, Jun, JunD, Fra1 and Myc siRNA and assayed for mRNA levels after 48 hours to confirm knockdown efficiency. **b,** Verification of siRNA functionality. K-Ras$^{G12D/+}$ MEFs were transfected with NT or Elk-1 siRNA and assayed for Elk-1 levels after 48 hours by western blot to confirm knockdown efficiency. **c,** Jun siRNA does not affect ROS levels in Jun$^{-/-}$ MEFs. Jun$^{-/-}$ MEFs were transfected with NT or Nrf2 siRNA and assayed for ROS by DCF oxidation after 48 hours. Results are representative of three independently performed experiments.

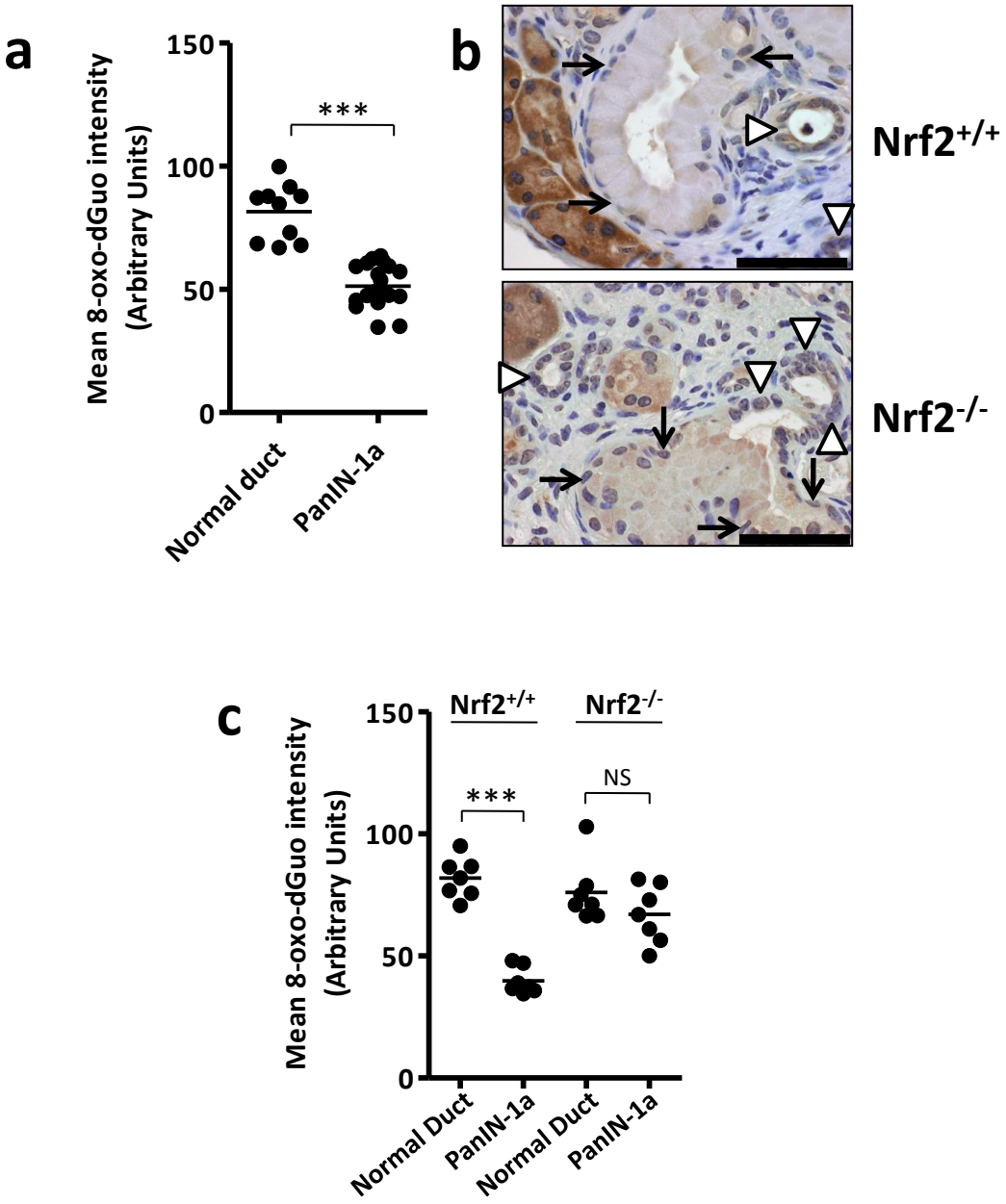

Supplementary Figure 11: Nrf2 promotes ROS detoxification in K-Ras mutant PanIN-1a. a, Quantification of mean 8-oxo-dGuo staining intensity in PanIN and normal ducts from Figure 4a. **b,** Decreased levels of lipid peroxidation in PanIN-1a, as determined by anti-malondialdehyde immunostaining, is Nrf2 dependent. Normal ducts (arrow heads), PanIN-1a (arrows). **c,** Quantification of mean 8-oxo-dGuo staining intensity in PanIN and normal ducts from Figure 4c. Scale bar = 56 microns.

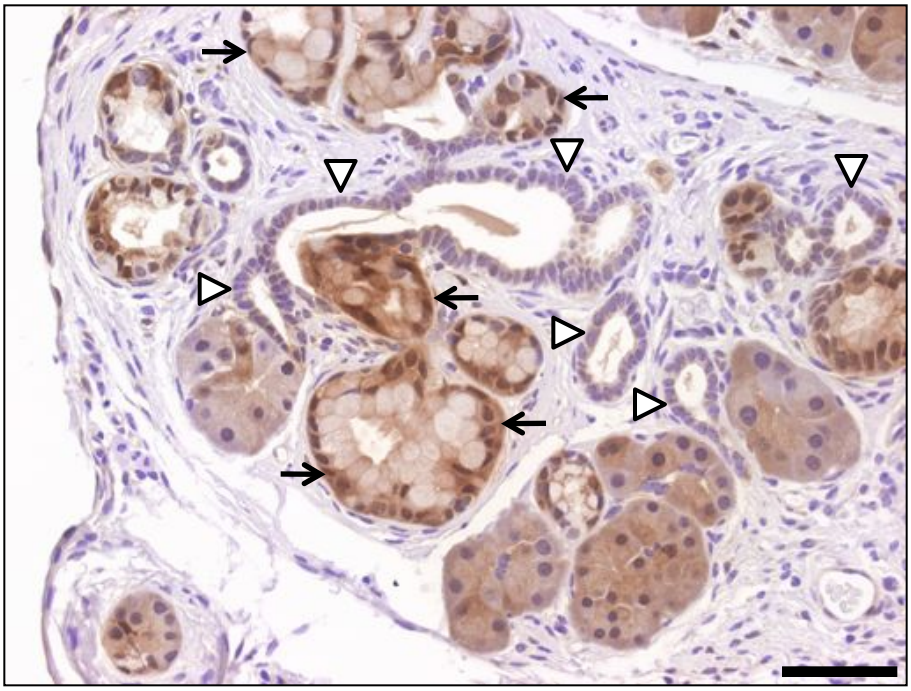

Supplementary Figure 12: K-Ras^{G12D} is most active in the preneoplastic but not morphologically normal appearing ductal cells. Elevated p-ERK immunostaining is observed in PanIN-1a but not normal adjacent ductal cells. Normal ducts (arrow heads), PanIN-1a (arrows). Scale bar = 56 microns.

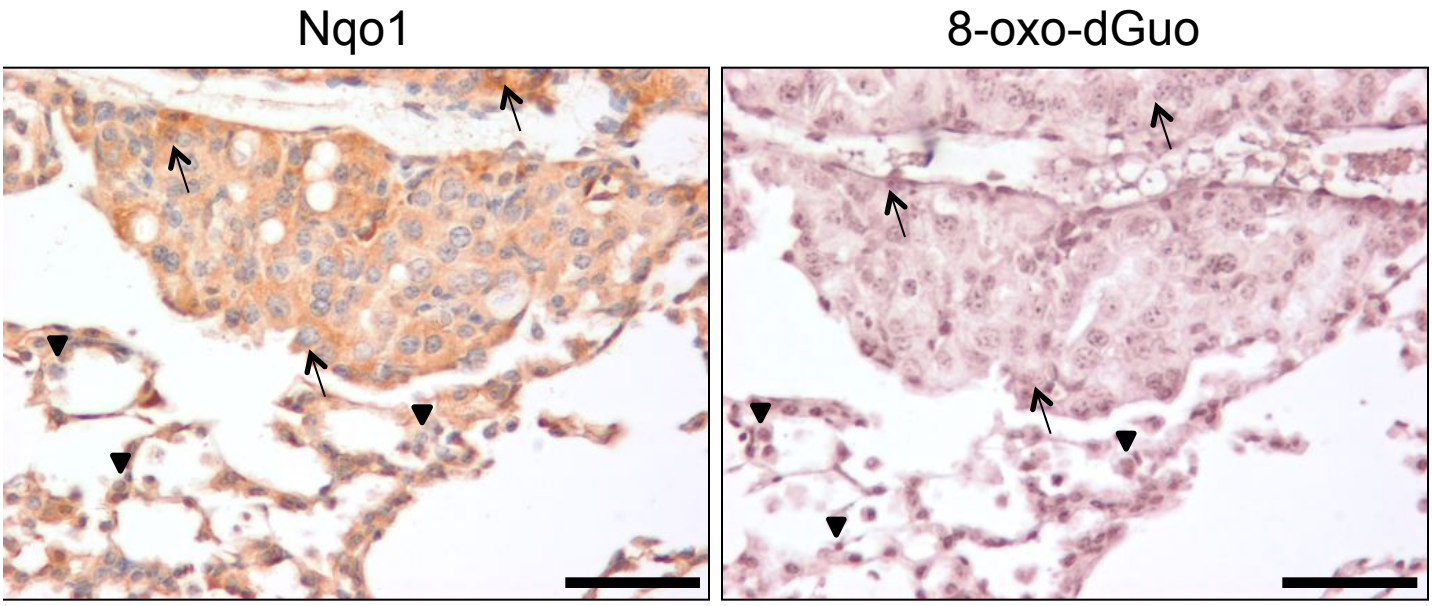

Supplementary Figure 13: Evidence for Nrf2 antioxidant program in B-Raf mutant lung adenomas. Nqo1 levels (left, brown staining) are elevated in adenomas compared to normal adjacent AT2 cells. 8-oxo-dGuo levels (right, purple staining) are lower in adenomas (arrows) compared to normal adjacent AT2 cells (arrowheads). Scale bar = 56 microns.

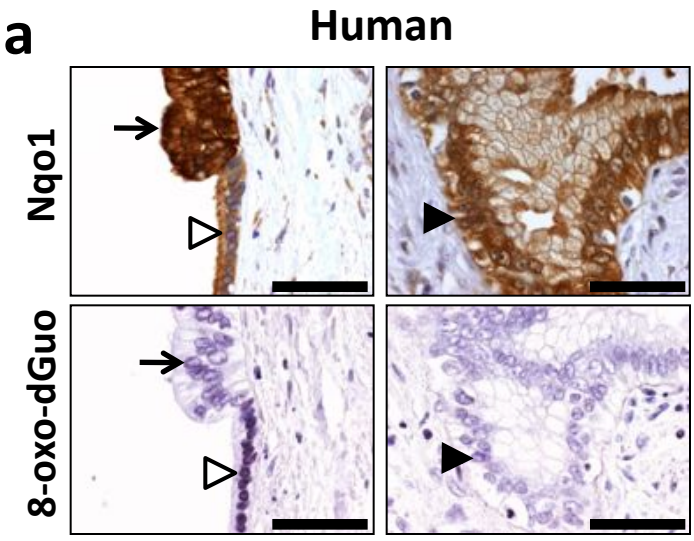

b

KEAP1	Somatic	Zygosity	K-Ras
G386R (ggc-gcg)	No	homozygous	G12D
L231 (insertion 8 bp)	Yes	homozygous	WT
T142M (acg-atg)	Yes	homozygous	G12V

Supplementary Figure 14: Evidence for Nrf2 antioxidant program in human pancreatic cancer. a, Nqo1 levels (brown staining) are elevated in human PanIN and PDA (11/11 of cases examined) compared to normal ducts. 8-oxo-dGuo levels (purple staining) are lower in PanIN and PDA compared to normal ducts, acinar cells and microenvironmental cell nuclei (11/11 of cases examined). PanIN (arrows), PDA (black arrowheads), normal ducts (white arrowheads). Scale bar = 56 μm. Samples are counterstained with hematoxylin. **b,** Paucity of somatic KEAP1 and Nrf2 mutations in human pancreatic cancer. 3 nonsynonymous KEAP1 mutations were found in over 100 cases analyzed, with only one somatic KEAP1 mutation occurring concomitantly with an oncogenic K-Ras allele.

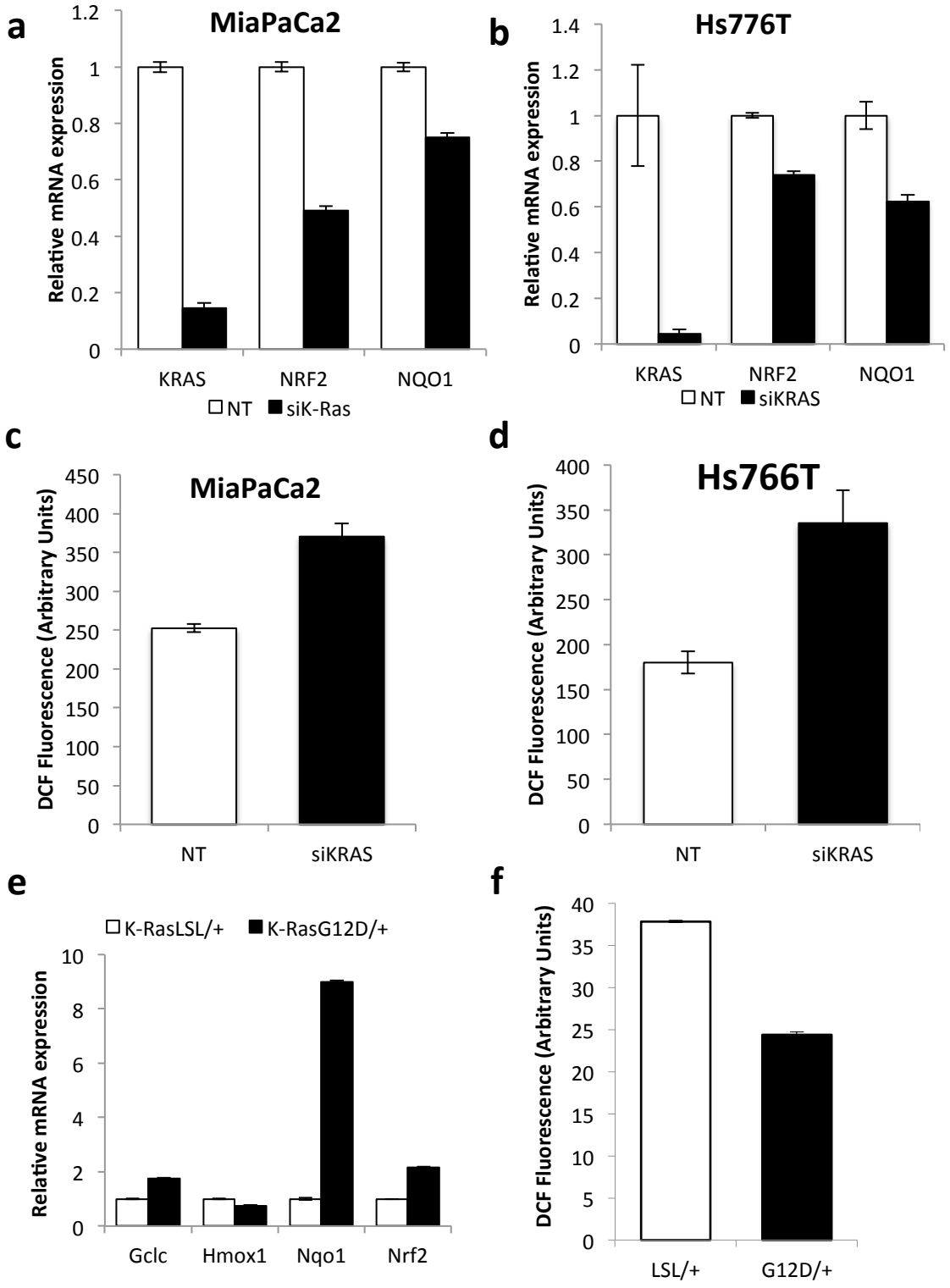

Supplementary Figure 15: **Oncogenic K-Ras regulates the Nrf2 antioxidant program in human and mouse pancreatic ductal cells. a-d,** K-RAS regulates NRF2 in human PDA cells. **a-b**, MiaPaCa2 cells (**a**) and Hs766T cells (**b**) were treated with K-RAS siRNA and NRF2 and NQO1 expression examined with taqman gene expression assays. **c-d,** ROS levels (DCF oxidation) were examined following K-RAS depletion with siRNA. **e-f,** K-Ras controls Nrf2 in murine pancreatic ductal epithelial cells. (**e**) LSL-K-Ras^{G12D} pancreatic ductal epithelial cells were infected with ad-mock (K-Ras$^{LSL/+}$) or ad-cre (K-Ras$^{G12D/+}$) and gene expression assayed with taqman gene expression assays. (**f**) ROS levels (DCF oxidation) were examined following expression of K-Ras^{G12D} in murine pancreatic ductal epithelial cells.

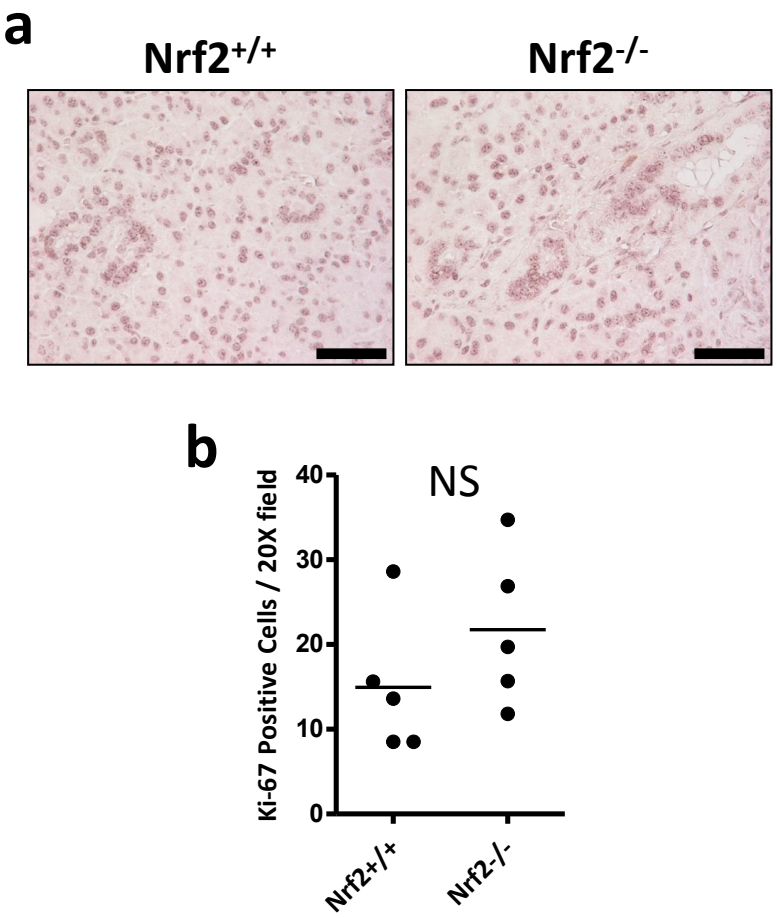

Supplementary Figure 16: Nrf2 deficiency does not affect 8-oxo-dGuo levels or proliferation in normal salivary gland. a, 8-oxo-dGuo immunostaining of salivary gland from $Nrf2^{+/+}$ and $Nrf2^{-/-}$ mice. **b,** Quantification of proliferation by Ki-67 immunostaining in the salivary gland from $Nrf2^{+/+}$ and $Nrf2^{-/-}$ mice.

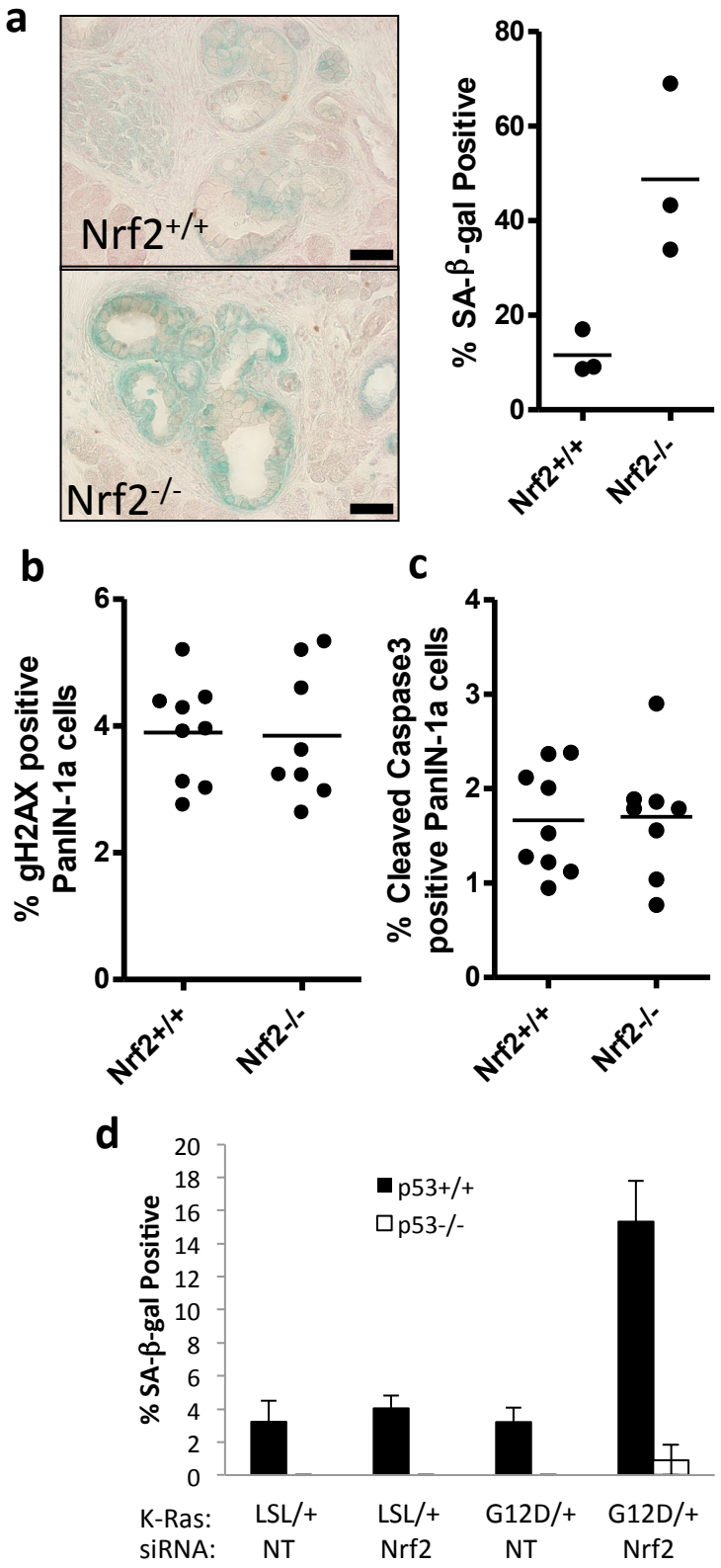

Supplementary Figure 17: Deficiency in Nrf2 results in senescence in vitro and in vivo. a, Quantification of senescence in Nrf2+/+ and Nrf2-/- PanIN. The content of senescent PanIN cells was denoted by the fraction exhibiting senescence-associated β-galactosidase (SA-β-gal) activity. **b,** Quantification of DNA damage, assayed with γH2AX immunostaining, in Nrf2+/+ and Nrf2-/- PanIN. **c,** Quantification of apoptosis, assayed by cleaved caspase 3 immunostaining, in Nrf2+/+ and Nrf2-/- PanIN. **d,** Acute depletion of Nrf2 with siRNA induces senescence selectively in K-Ras$^{G12D/+}$ MEFs but not K-Ras$^{LSL/+}$ MEFs. Senescence was not observed upon Nrf2 depletion in p53$^{-/-}$; K-Ras$^{G12D/+}$ MEFs. Senescence was determined by senescence-associated β-galactosidase (SA-β-gal) activity.

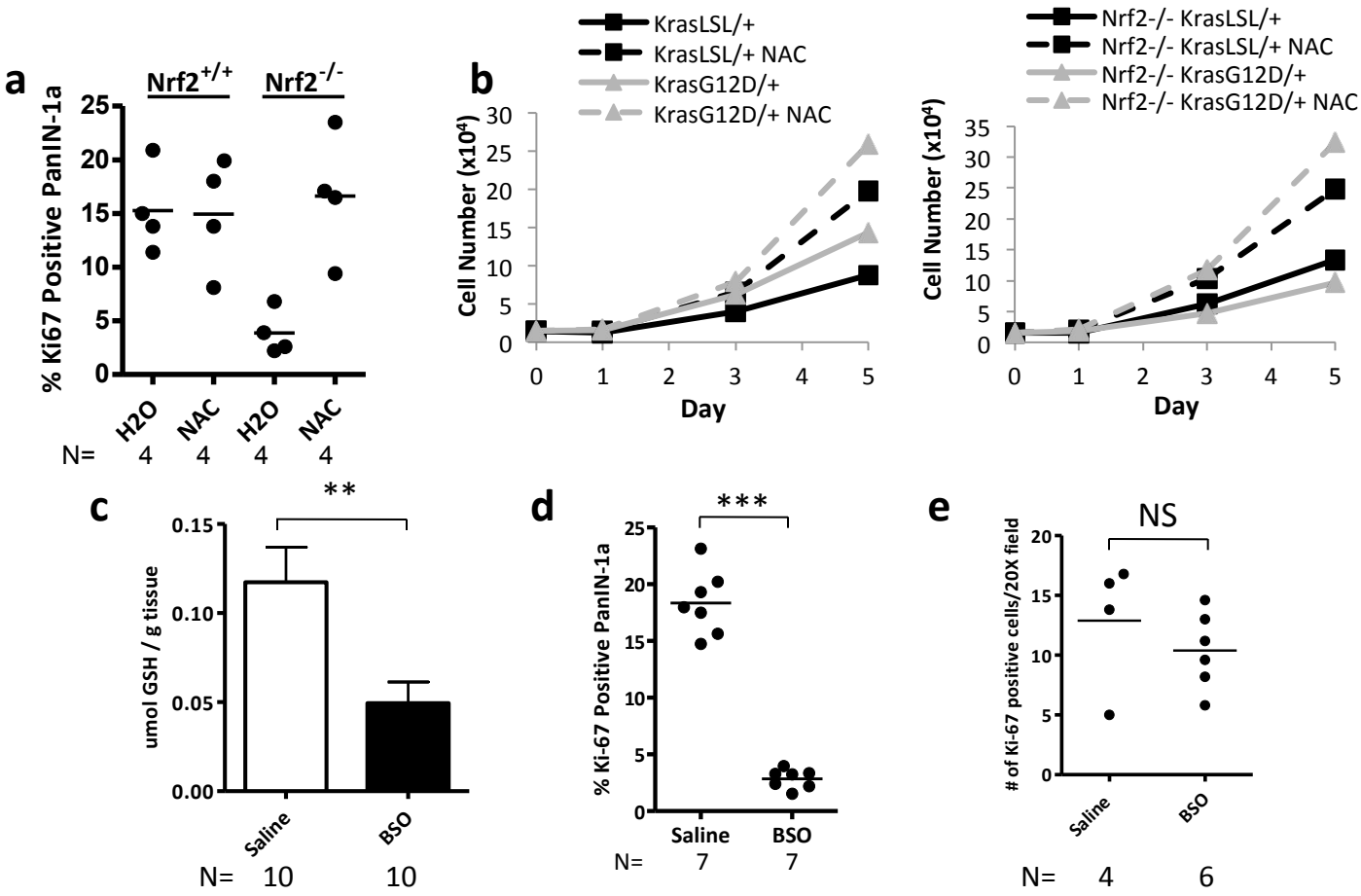

Supplementary Figure 18: The intracellular redox state regulates proliferation in cells expressing K-Ras^{G12D}. a-b, N-acetyl cysteine rescues the proliferation defect of Nrf2$^{-/-}$; K-Ras$^{G12D/+}$ cells. **a,** Treatment with 30mM NAC in the drinking water rescues the decrease in proliferation observed in Nrf2-/- PanIN-1a. 9 month old mice were treated for 7 days with NAC and proliferation determined by Ki-67 immunostaining. **b,** Proliferation of K-RasLSL/+ and K-RasG12D/+ (left) and K-RasLSL/+; Nrf2-/- and K-RasG12D/+; Nrf2-/- MEFs (right) in response to 2mM N- acetyl cysteine (NAC). **c-e,** Glutathione depletion inhibits PanIN-1a proliferation, but not proliferation of adjacent normal pancreas. **c,** 10mmol/kg BSO i.p. depletes glutathione in the mouse pancreas. Wild-type mice were treated daily for 7 days and pancreas glutathione determined. **d,** Treatment with BSO decreases proliferation in PanIN-1a as determined by Ki-67 immunostaining. **e,** BSO treatment does not affect proliferation in normal adjacent pancreas. The number of Ki-67-positive cells / 20X field was determined to be similar between saline and BSO treated adjacent normal pancreas.

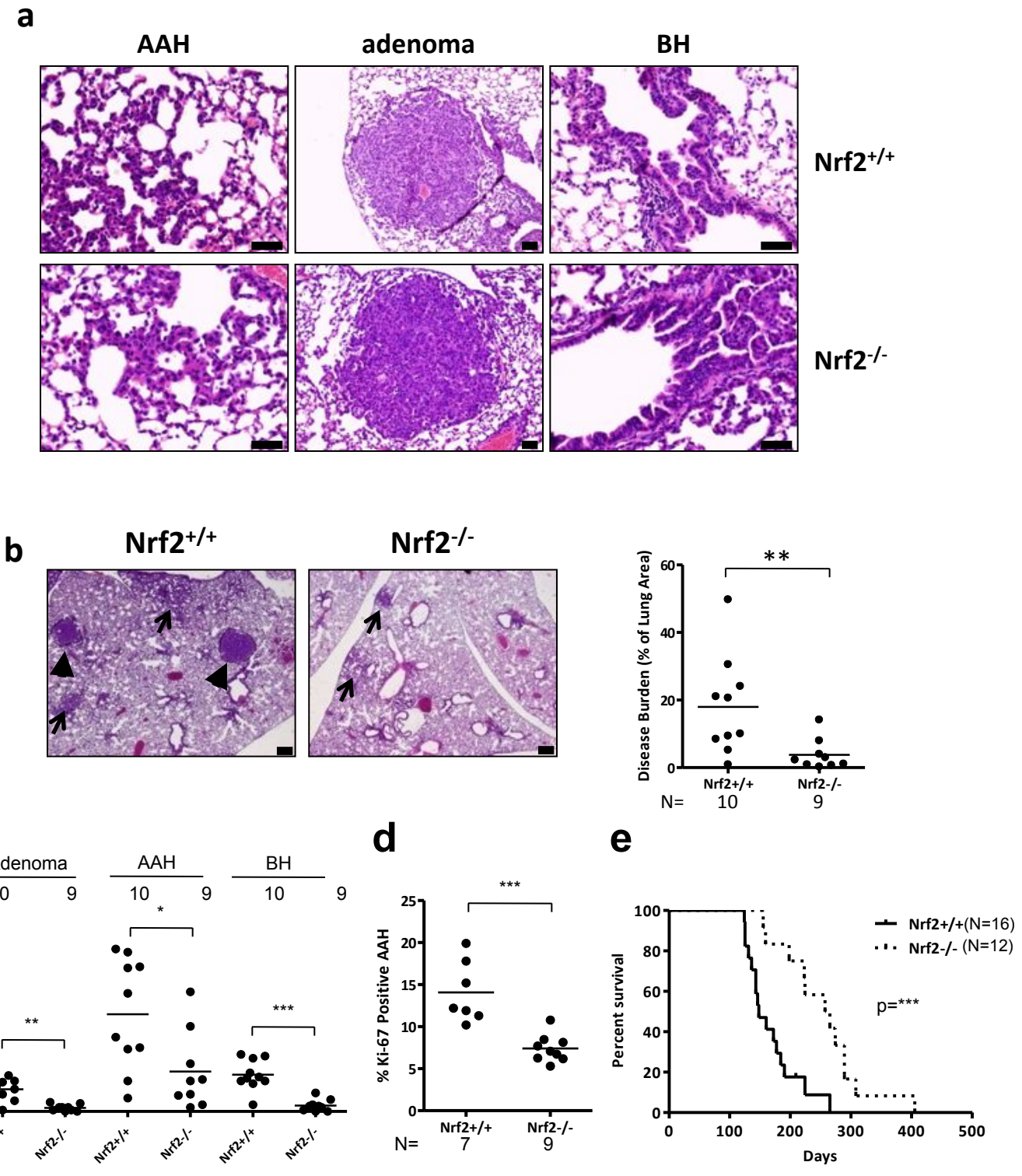

Supplementary Figure 19: Nrf2$^{-/-}$ mice demonstrate a reduction in K-Ras^{G12D}-mediated lung tumorigenesis. a, H&E images of adenomatous alveolar hyperplasia (AAH), adenomas, and bronchiolar hyperplasia (BH) from Nrf2$^{+/+}$ and Nrf2$^{-/-}$ mice. **b,** Nrf2$^{-/-}$ mice demonstrate a reduction in lung disease burden compared to Nrf2$^{+/+}$ mice. **c,** Characterization of the spectrum of pulmonary preneoplasms. Nrf2$^{-/-}$ mice develop significantly fewer adenomas, adenomatous alveolar hyperplasia (AAH) and bronchiolar hyperplasia (BH) than Nrf2$^{+/+}$ mice. **d,** Proliferation of cells in AAH was decreased in Nrf2$^{-/-}$ compared to Nrf2$^{+/+}$ mice. **e,** Nrf2$^{-/-}$ mice demonstrate increased survival compared to Nrf2$^{+/+}$ mice following expression of K-Ras^{G12D} (median survival 261 vs. 148 days, respectively). Number of mice denoted in each figure.

Supplementary Discussion

NFE2L2, KEAP1, KRAS sequencing

The transcriptional upregulation of Nrf2 by oncogenic K-Ras is an additional genetic mechanism to activate this antioxidant pathway from the previously described somatic mutations in Keap1 and Nrf2 that stabilize Nrf2 protein. The existence of concomitant somatic mutations in K-Ras and Nrf2/Keap1 would therefore be redundant and may lack selective pressure to evolve in tumors that harbor oncogenic K-Ras mutations as the initiating event, such as PDA. A large series of over 100 samples of xenografted primary PDA and additional pancreatic cancer cell lines known to lack microsatellite instability were analyzed for mutations in *KRAS*, *NFE2L2* (NRF2) and *KEAP1*. KRAS mutations were found in all but 6 cases, consistent with published reports [1]. No mutations of the KEAP1-binding site in NRF2 were identified, in contrast to several *NFE2L2* mutations recently reported in lung and head and neck cancers[2]. LOH of the *KEAP1* locus at 19p13.2 was noted in 33 of the xenografts and 13 of the cell lines. Sequencing of *KEAP1* in these samples revealed three cases harboring non-synonymous alterations in the published *KEAP1* sequence. The first alteration, G386R, was present in the germline of this individual and although it could potentially affect NRF2 recognition, its functional significance is unknown. The second mutation, L231, is predicted to result in a frame shift and a truncated KEAP1 protein and therefore should result in NRF2 activation. Interestingly, this case harbors a wild-type KRAS allele. The final alteration was a somatic mutation (T142M) that affects a highly conserved threonine residue in the BTB (Bric-a-Brac)/POZ domain thought to control the redox sensitive regulation of NRF2[3]. Therefore, no *NFE2L2* mutations and only one somatic mutation in *KEAP1* was noted in over 100 PDA cases that contained oncogenic *KRAS* mutations, yielding a coexisting mutational prevalence (~1%) that is much lower than any other tumor type reported to date.

Supplemental References

1. Almoguera, C*., et al.* Most human carcinomas of the exocrine pancreas contain mutant c-K-ras genes. *Cell* **53**, 549-554 (1988).
2. Shibata, T*., et al.* Cancer related mutations in NRF2 impair its recognition by Keap1-Cul3 E3 ligase and promote malignancy. *Proc Natl Acad Sci U S A* **105**, 13568-13573 (2008).
3. Zipper, L.M. & Mulcahy, R.T. The Keap1 BTB/POZ dimerization function is required to sequester Nrf2 in cytoplasm. *J Biol Chem* **277**, 36544-36552 (2002).